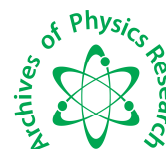




Scholars Research Library

Archives of Physics Research, 2015, 6 (5):17-28
(<http://scholarsresearchlibrary.com/archive.html>)



Scholars Research
Library

ISSN : 0976-0970

CODEN (USA): APRRC7

Transport properties of iron doped bismuth silicate glass ceramics

Rajesh Parmar

Department of Physics, Maharishi Dayanand University, Rohtak, Haryana, India

ABSTRACT

The glass ceramics of various compositions $60\text{SiO}_2.(40-x)\text{Bi}_2\text{O}_3.x\text{Fe}_2\text{O}_3$ with $x = 0, 1, 2, 3, 4$ and 5 were prepared by annealing the as prepared glasses at temperature $\sim 50^\circ\text{C}$ above the glass transition temperature (T_g), in the electrically heated furnace and then hold the temperature constant for one hour. The ac conductivity of different compositions of iron doped bismuth silicate glass ceramics were studied in the wide temperature range 533 K to 713 K and frequency range 10^1 Hz to 1 MHz . The temperature and frequency dependent conductivity was found to obey Jonscher's power law all the compositions and found to increase with increase in Fe_2O_3 content. Various parameters like dc conductivity (σ_{dc}), cross-over frequency (ω_H) and frequency exponent (S) were estimated from theoretical fitting of experimental data of ac conductivity with Jonscher's power law, which showed very good agreement for all the compositions. Enthalpy to dissociate the cations from original site to a charge compensating center (H_f) and enthalpy of migration (H_m) had also been estimated. The conductivity data were analyzed in terms of different theoretical models to determine the possible conduction mechanism. Analysis of the conductivity data and the frequency exponent 'S' showed that the correlated barrier hopping of electrons between Fe^{2+} and Fe^{3+} ions in the glass ceramics was suitable to describe the conduction mechanism for ac conduction. The temperature dependent dc conductivity were analyzed using the theoretical variable range hopping model (VRH) proposed by Mott which describe the hopping conduction in disordered semiconducting glass in low temperature range. The various polaron hopping parameters were also calculated. Greave's VRH model was found to be in good agreement with experimental data.

INTRODUCTION

Oxide glasses containing transition metal ions (TMIs) such as Ti, Fe, and V etc. are of great interest because of their semiconducting properties [1-12]. The semiconducting properties of these glasses arise from the presence of TMI in multivalent states and electrical conductivity in general is controlled by hopping of electrons or small polarons from low valence state to high valence state of transition metal ion [13-14] e.g. in glasses containing iron, the electronic conduction occurs is due to the hopping of a 3d electron from the Fe^{2+} to Fe^{3+} ion. These glasses are also interesting due to their technological applications in electrical and optical memory switching devices [1,7], cathode materials in battery [15] and in field of tunable lasers, solar energy convereters, fiber optics telecommunication devices[16]. Glasses containing iron are found to have high electrical conductivity at room temperature and are find useful applications as a sensor in magneto-resistance effect [17].The addition of TMI, like iron, to the bismuth silicate glasses is expected to improve their electrical and dielectric features. The conductivity of bismuth silicate [18-21] and bismuth iron glasses [22- 25] has been studied in detail by many researchers, but there is hardly any report on electronic transport of iron bismuth silicate glass ceramics The aim of the present paper is to probe the frequency and temperature dependence of ac conductivity of iron doped bismuth silicate glass ceramics and to understand the conduction mechanism.

MATERIALS AND METHODS

The glass compositions $60\text{SiO}_2 \cdot (40-x)\text{Bi}_2\text{O}_3 \cdot x\text{Fe}_2\text{O}_3$ with $x = 0, 1, 2, 3, 4$ and 5 were prepared using the standard melt quenching technique as reported elsewhere [26]. The thermal stress of the prepared glass samples were removed by annealing them for 8 hours at temperature about 400°C and then cooled to room temperature. Based on the DSC data, the glass ceramics of these samples were prepared by annealing the as prepared glasses at temperature $\sim 50^\circ\text{C}$ above the glass transition temperature (T_g), in the electrically heated furnace and then hold the temperature constant for one hour. The samples were allowed to cool normally and were taken out from the furnace at the room temperature. The crystalline nature of prepared glass ceramics was confirmed by the presence of sharp peaks in X-ray diffraction patterns of the powdered samples recorded by using a Rigaku Table-top X-ray diffractogram with $\text{CuK}\alpha$ radiation ($\lambda=1.54\text{\AA}$). For electrical measurements, samples were cut into small size and polished, both sides of the samples were coated with a thin layer of silver paint to serve as electrodes. The conductivity measurements were carried out by using Alpha-A high Resolution Dielectric, Conductivity, Impedance and Gain Phase Modular Measurement System Novocontrol Technologies GmbH & Co. KG in the frequency range 10^{-1} Hz to 1MHz ranging the temperature range 533 K to 713 K. The fitting of experimental data was done using linear and non-linear fit modules of Origin Pro 8.6 software.

RESULTS AND DISCUSSION

3.1 AC conductivity

The ac conductivity of different glass ceramic compositions $60\text{SiO}_2 \cdot (40-x)\text{Bi}_2\text{O}_3 \cdot x\text{Fe}_2\text{O}_3$ with $x = 0, 1, 2, 3, 4$ and 5 has been studied in temperature range 533 K to 713 K and frequency range 10^{-1} Hz to 1MHz, show similar frequency and temperature dependence. It is found to increase with increase in Fe_2O_3 content. The compositional and frequency dependent conductivity ($\sigma'(\omega)$) goes on increasing with increase in Fe_2O_3 content for the studied frequency range at any particular temperature. A typical graph showing variation of $\sigma'(\omega)$ with frequency at 673 K is shown in Fig.1. The similar trend is observed by some other researchers [23,24] and for glass compositions of presently studied glass ceramics compositions. The variation of $\sigma'(\omega)$ with frequency in case of glass samples with $x = 3, 4$ and 5 shows double plateau for temperatures above 633K, 573K and 493K respectively, whereas such plateau is not obtained in any studied glass ceramics samples. Perusal of data presented in Fig.1 shows that the crystallization of glass compositions $\sigma'(\omega)$ shows an increase for compositions with $x = 0, 1, 2$ and 3 whereas it remains almost same for ceramics compositions with $x = 4$ and 5 . The frequency dependent conductivity ($\sigma'(\omega)$) of glass ceramics samples, presented in Fig.1, is characterized by two regions: (i) a plateau region and (ii) dispersion region. Plateau region is observed at low frequencies, where random distribution of the charge carriers via activated hopping give rise to a frequency-independent conductivity. With increase in temperature, width (frequency range) of this region goes on increasing. The curves are flat in low frequency region as the conductivity values approximately correspond to σ_{dc} . On the other hand, dispersive region is observed at higher frequencies, where $\sigma'(\omega)$ shows high dependence on frequency and increases with increase in ω . The conductivity graph become more dispersive with increase in frequency and tend to merge in high frequency regime as the width of dispersive region decreases with increases in temperature exhibiting the weak temperature dependence.

The changeover of conductivity is shifted towards higher frequencies with increase in temperature because mobile ions acquire more thermal energy and cross the barrier more easily [25]. In other words, when temperature is increased the dispersion starts at higher frequency. Generally, ac conductivity behavior is analyzed using Jonscher's power law [11, 12, 20, 21,30-32],

$$\sigma'(\omega) = \sigma_{dc} \left[1 + \left(\frac{\omega}{\omega_H} \right)^s \right] \quad (1)$$

where σ_{dc} is the (frequency independent) dc conductivity, ω_H is crossover frequency of the charge carriers ions separating dc regime (plateau region) from the dispersive conduction and s 's frequency exponent that lies between 0.6 and 1 [31,33]. The exponent s is attributed to the interaction between the charge carrier ions with the frame work carrying the balancing charge and its smaller value signifies higher degree of modification [29]. The values of σ_{dc} , ω_H and s are obtained by the fitting of the experimental data of frequency dependent conductivity ($\sigma'(\omega)$) measured at different temperatures with Eq. (1). As shown in Fig.2, the experimental data fitted with Jonscher's universal power law (Eq.1) for glass ceramic composition with $x = 5$, gives very good fitting with best parameters

fit, R^2 , in the range 0.9914 – 0.9992 and error factor of least square fit, Chi^2 , lying in the range of 1.0574×10^{-14} – 9.824×10^{-16} and is observed to be obeyed in all the presently studied glass ceramic compositions. So, ac conduction in the presently studied glass ceramic compositions may be attributed to hopping mechanism and is found to be consistent with the observed in many other semiconducting glasses [11, 21, 29, 30, 34]. The increase in electrical conductivity with the increase in temperature is due to the increase in drift mobility of the thermal activated charge carriers [28, 35].

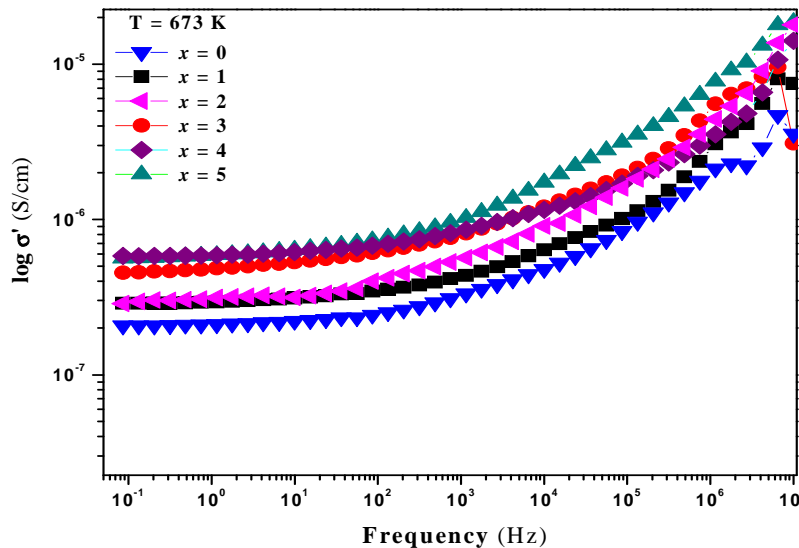


Fig.1 Compositional and frequency dependence of total ac conductivity (σ' (ω)) of glass ceramics system $60\text{SiO}_2.(40-x)\text{Bi}_2\text{O}_3.x\text{Fe}_2\text{O}_3$ at $T=673\text{ K}$

When the conduction occurs via defect mechanism then at a given instant only a fraction (n) of total charge carriers (N) are mobile, which is given by [11,36]

$$n = N \exp\left(-\frac{G_f}{kT}\right) = N \exp\left(\frac{S_f}{k}\right) \times \exp\left(-\frac{H_f}{kT}\right) \tag{2}$$

where S_f , H_f and G_f are entropy, enthalpy and free energy, respectively, to dissociate the cation from its original site next to a charge compensating centre. The crossover frequency (ω_H) and dc conductivity (σ_{dc}) are given by [36]

$$\omega_H = \omega_o \exp\left(\frac{S_m}{k}\right) \times \exp\left(-\frac{H_m}{kT}\right) \tag{3}$$

and

$$\sigma_{dc} = \frac{NZ^2 e^2 d^2 \gamma \omega_o}{kT} \exp\left(\frac{S_f + S_m}{k}\right) \times \exp\left(-\frac{H_f + H_m}{kT}\right) \tag{4}$$

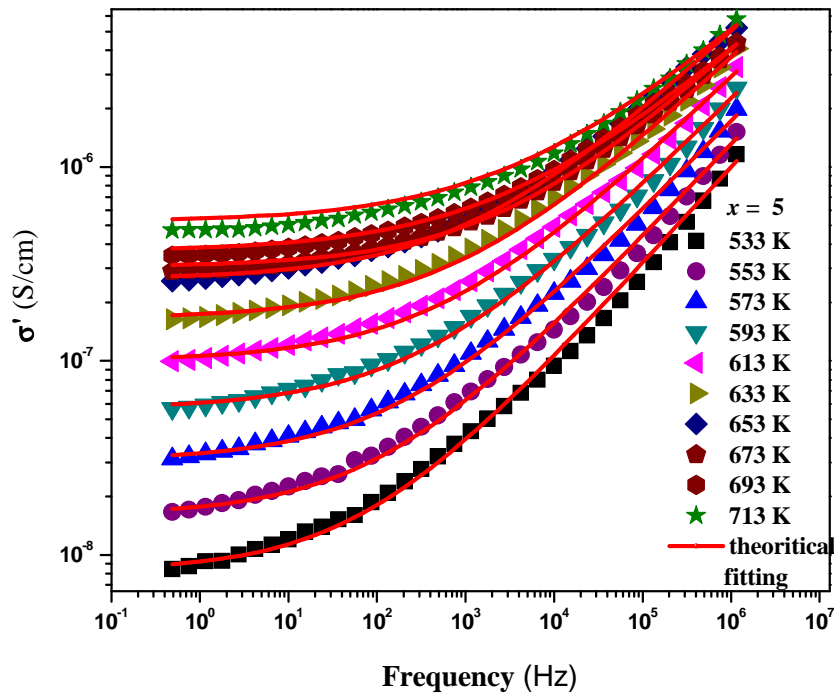


Fig.2 Measured total ac conductivity ($\sigma'(\omega)$) of glass ceramic compositions $60\text{SiO}_2.(40-x)\text{Bi}_2\text{O}_3.x\text{Fe}_2\text{O}_3$ with $x = 5$, shown as a function of frequency at ten different temperatures. The solid line in the figure are the best fits obtained from fitting of experimental data with Jonscher's power law

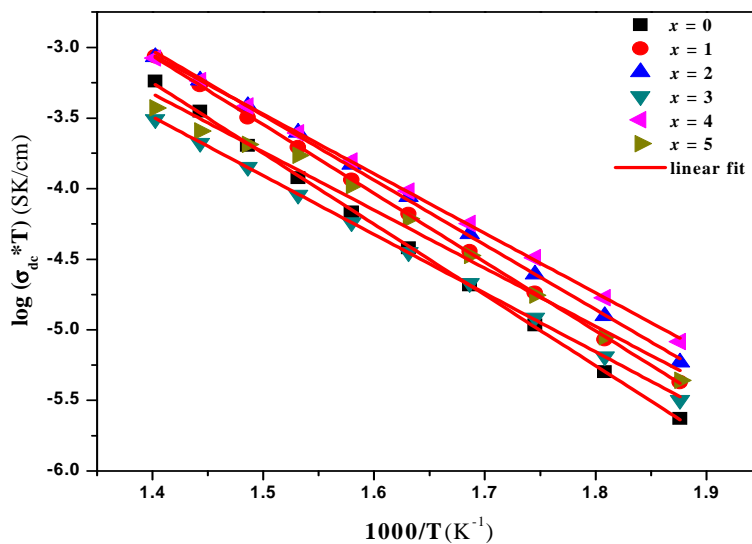


Fig.3 Linear fit of $\log(\sigma_{dc} T)$ versus $1/T$ glass ceramics compositions $60\text{SiO}_2.(40-x)\text{Bi}_2\text{O}_3.x\text{Fe}_2\text{O}_3$ where σ_{dc} is dc conductivity and T is absolute temperature

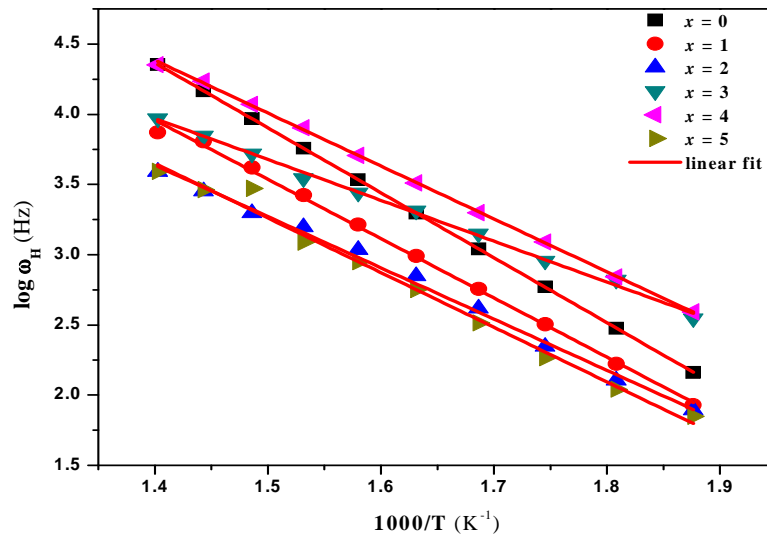


Fig.4 Linear fit of $\log \omega_H$ versus $1/T$ glass ceramics compositions $60\text{SiO}_2 \cdot (40-x)\text{Bi}_2\text{O}_3 \cdot x\text{Fe}_2\text{O}_3$

where ω_H is crossover frequency and T is absolute temperature

From Eqs (3) and (4) it is clear that the slopes of plots of $\log(\sigma_{dc}T)$ and $\log \omega_H$ versus $1/T$ would be $H_f + H_m$ and H_m respectively. The slopes of plots $\log(\sigma_{dc}T)$ and $\log \omega_H$ versus $1/T$ shown in Figs.(3) and (4) are estimated using linear fitting. Both the plots show linearity for all the compositions $60\text{SiO}_2 \cdot (40-x)\text{Bi}_2\text{O}_3 \cdot x\text{Fe}_2\text{O}_3$. The values of $H_f + H_m$ and H_m as calculated from the slopes are presented in Table 1. Perusal of the data presented in Table 1, shows that $H_f > 0$, for all glass ceramic samples, and therefore, on addition of Fe_2O_3 to bismuth silicate glass ceramic system, it is found that number of mobile charge carriers at any instant becomes less than total number of charge carriers [11]. Whereas, the conductivity of glass ceramic samples is observed to increase with increase in Fe_2O_3 content (as shown in Fig.1). The increase in conductivity may either be due to increase in mobility of charge carriers on addition of Fe_2O_3 or increase in number of mobile charge carriers.

TABLE. 1. Enthalpy to dissociate the cation from its original site next to a charge compensating center (H_f), enthalpy of migration (H_m) of $60\text{SiO}_2 \cdot (40-x)\text{Bi}_2\text{O}_3 \cdot x\text{Fe}_2\text{O}_3$ of glass ceramic with different values of x

Parameters	$x=0$	$x=1$	$x=2$	$x=3$	$x=4$	$x=5$
$H_f+H_m(\text{eV})(\pm 0.001\text{eV})$	0.995	0.967	0.910	0.826	0.837	0.818
$H_m(\text{eV})(\pm 0.001\text{eV})$	0.919	0.839	0.725	0.578	0.748	0.773
$H_f(\text{eV})(\pm 0.001\text{eV})$	0.076	0.128	0.185	0.248	0.089	0.045

3.1.1. Variation of Frequency Exponent and Conduction Mechanism

The conduction mechanism in any material could be understood from the temperature dependent behaviour of frequency exponent (s). To interpret the electrical conduction mechanism in the materials, various models based on classical hopping of charge carriers over barrier, quantum mechanical tunneling and the overlapping large-polaron tunneling, [37-42] have been proposed on the basis of variation of frequency exponent with temperature and frequency. The temperature dependence of frequency exponent (s), obtained from fitting of experimental data with Eq.(1) is shown in Fig. 5.

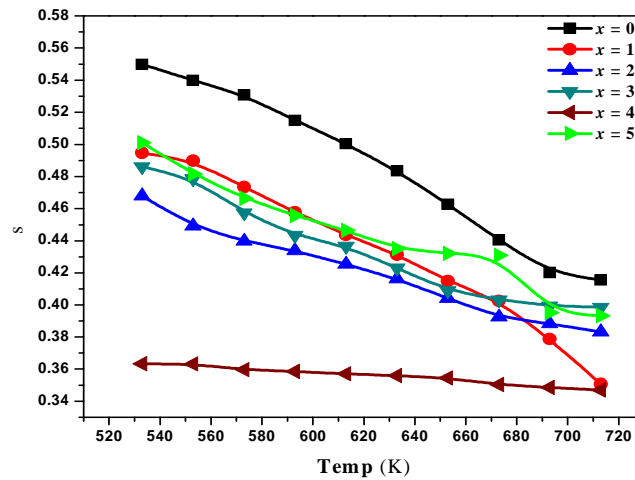


Fig.5. The variation of frequency exponents (s) for different $60\text{SiO}_2.(40-x)\text{Bi}_2\text{O}_3.x\text{Fe}_2\text{O}_3$ glass ceramics compositions are shown as a function of temperature, obtained from fitting of experimental data of total ac conductivity with Jonscher's power law

The variation of ' s ' with temperature correlates the ac conductivity mechanism as discussed below [20]

- (1) If ' s ' depends upon frequency but is independent of temperature then the conduction mechanism can be explained by the quantum mechanical electron tunneling theory.
- (2) If ' s ' increases with increase in temperature, then the conduction process can be explained with the small polaron quantum mechanical tunneling theory whereas if ' s ' decreases at first, reaching a minimum and increases thereafter with increase temperature then it can be explained by large polaron quantum mechanical tunneling model.
- (3) If ' s ' decreases with temperature then it follows correlated barrier hopping (CBH) conduction mechanism.

It is noted that for all glass ceramic samples, frequency exponent ' s ' decreases with increase in temperature. In the present glass ceramic system, CBH conduction mechanism is predominant. The Correlated Barrier Hopping (CBH) model, proposed by Elliot, [38-41] has also been applied to glassy semiconductors. In this model, the charge transport occurs between localized states due to hopping over the potential barriers and for neighboring sites at a separation R , the coulomb wells overlap, resulting in lowering of effective barrier height from W_m to W , which for single electron hopping is given by

$$W = W_m - \frac{e^2}{\pi \epsilon' \epsilon_o R} \quad (5)$$

Where W_m is barrier height at infinite site separation, ϵ' is dielectric constant of material, ϵ_o is the permittivity of free space and R is the distance between two hopping sites. The maximum barrier height, W_m is also called polaron binding energy. The ac conductivity and frequency exponent, ' s ' as per this model are given by [26,35]

$$\sigma(\omega) = \frac{\pi^2}{24} N^2 \epsilon' \epsilon_o \omega R_\omega^6 \quad (6)$$

$$\text{and} \quad s = 1 - \frac{6k_B T}{W_m + k_B T \ln(\omega \tau_o)} \quad (7)$$

where N is the concentration of the charge carriers, τ_o is relaxation time and R_ω is the hopping length at frequency ω . It is clear from the Eq.(7) that s decreases with increase in temperature, which is consistent with the behavior of ' s ' (obtained from fitting of experimental data with the Eq.(1) Jonscher's universal power law as shown in Fig.6)

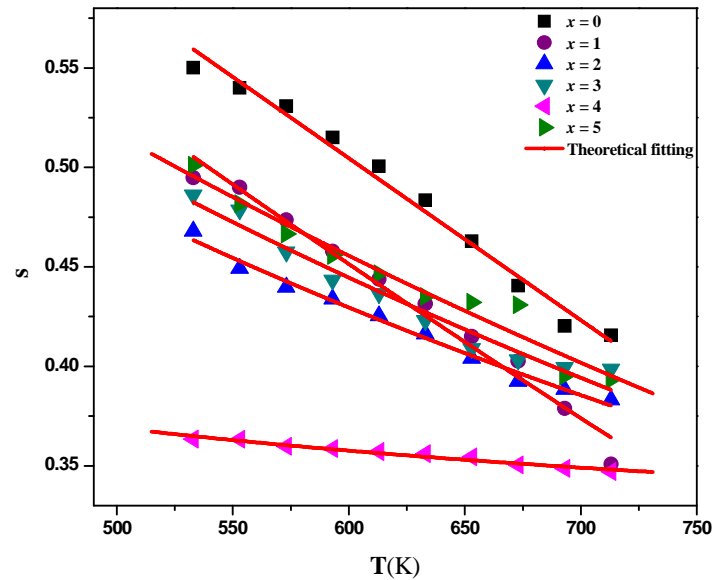


Fig.6 The variation of frequency exponent (s) for different 60SiO₂.(40-x)Bi₂O₃.xFe₂O₃ glass ceramics compositions are shown as a function of temperature

This suggests that the conductivity behavior of iron doped bismuth silicate glass ceramics can be explained using CBH model. Similar type of variation of ‘s’ with increase in temperature has also been reported by Pike [43], Elliott [38] and Springett [44] in different glass ceramics containing transition metal ions (TMIs). The observed variation of ‘s’ with temperature may be due to different contributions from conducting and dielectric losses at different temperatures[45, 46]. The values of maximum barrier height (W_m) and relaxation time (τ_o) have been estimated from the fitting of frequency exponent (obtained from the fitting of $\sigma'(\omega)$ with Jonscher's power law) with CBH model (Eq. (7)) by keeping $\omega = 2\pi$ MHz (i.e 1MHz) and are listed in Table 2. Perusal of data presented in Table 2, it is observed that W_m decreases with increase in Fe₂O₃ content. The values of band gap energy estimated from the optical data lies between 2.88 and 3.40 eV and it also decreases with increase in Fe₂O₃ content. The variation in values of activation energy and band gap energy are in accordance with the decrease in values of barrier height at infinite separation.

Table 2. Maximum barrier height at infinite separation (W_m) and relaxation time (τ_o) estimated from fitting of Eq.(5.4), Concentration of Fe -ions (N), Mean spacing between Fe-ions (R), Polaron radius (r_p), Activation energy (W), Band gap energy(E_g), Density of states at Fermi level ($N(E_f)$) and inverse localization length (α) of glass ceramics compositions 60SiO₂.(40-x)Bi₂O₃.xFe₂O₃ with different values of x

Physical Parameters	x = 0	x = 1	x = 2	x = 3	x = 4	x = 5
W_m (eV)	0.619	0.490	0.273	0.325	0.443	0.359
τ_o (μ s)	0.184	0.690	29.993	14.542	786.600	9.451
N ($\times 10^{21}$ cc)	----	0.349	0.704	1.063	1.429	1.801
R(Å)	----	14.192	11.236	9.797	8.877	8.219
r_p (Å)	----	5.719	4.528	3.948	3.577	3.312
W (eV)	0.942	0.914	0.857	0.773	0.784	0.765
E_g (eV)	3.40	3.31	3.24	3.00	2.90	2.88
$N(E_f)$ ($\times 10^{20}$ eV ⁻¹ cm ⁻³)	----	0.913	1.963	3.284	4.350	5.622
α (Å^{-1})[By Greave's model]	----	0.585	0.692	0.716	0.801	0.841

3.2.DC conductivity

The dc conductivity (σ_{dc}) of $60\text{SiO}_2.(40-x)\text{Bi}_2\text{O}_3.x\text{Fe}_2\text{O}_3$ glass ceramics compositions is obtained from the fitting of the experimental data of frequency dependent conductivity ($\sigma'(\omega)$) at different temperatures with Jonscher's power law (Eq.1) is shown in Fig. 7 and it is observed to lie in the range from 10^{-8} to 10^{-6} S cm^{-1} . Further, the frequency dependent conductivity curves (as in Fig.2) are characterized by well-defined plateau, where the conductivity is identical to the dc conductivity. Both the values of the dc conductivity, one obtained by fitting with Eq. (1) and the other from plateau of $\sigma'(\omega)$ versus ω plot, are almost the same.

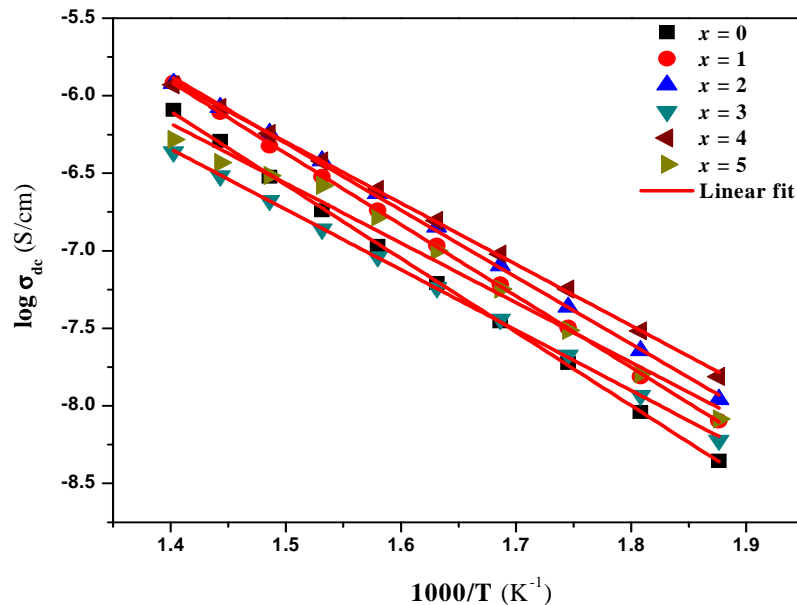


Fig.7 Variation of dc conductivity versus reciprocal of temperature for different glass ceramics compositions $60\text{SiO}_2.(40-x)\text{Bi}_2\text{O}_3.x\text{Fe}_2\text{O}_3$

The inverse temperature variation of dc conductivity follows the Arrhenius relation [28]

$$\sigma_{dc} = \sigma_o \exp\left[-\frac{W}{kT}\right] \quad (8)$$

where σ_o is the pre-exponential parameter which depends on semiconductor nature, W denotes the thermal activation energy of electrical conduction, and k is Boltzmann's constant. The variation of $\log \sigma_{dc}$ with $1000/T$ is shown in Fig. 7 for compositions with $x = 0, 1, 2, 3, 4$ and 5 . The activation energy (W) is calculated from the slope of linear fit of $\log \sigma_{dc}$ versus $1000/T$ plot. The values of activation energies (W) are presented in Table 2 for all the samples. The activation energy is observed to decrease indicating thereby the increase in conductivity with the increase in concentration of Fe_2O_3 . The activation energy corresponds to the trap level located below the conduction band. It is observed that band gap energy decreases with the increase in concentration of Fe_2O_3 . The decrease in activation energy is found to be consistent with decrease in band gap energy on increasing Fe_2O_3 .

The concentration of iron ions (N) has been estimated using the following relation [12]

$$N = 2dN_A \left[\frac{W_{\text{Fe}_2\text{O}_3}}{M_{\text{Fe}_2\text{O}_3}} \right] \quad (9)$$

where d is the density, $M_{Fe_2O_3}$ is molecular weight of Fe_2O_3 , $W_{Fe_2O_3}$ is weight fraction of Fe_2O_3 and N_A is Avogadro's number. The correlation between N and mean spacing between any two Fe-ions (R) is generally described [12] as

$$R = \left[\frac{1}{N} \right]^{\frac{1}{3}} \quad (10)$$

Using above relations, the polaron radius (r_p) is given by [12]

$$r_p = \frac{1}{2} \left[\frac{\pi}{6} \right]^{\frac{1}{3}} R \quad (11)$$

The density of states, $N(E_F)$, for thermally activated electron hopping near the Fermi level is calculated by the relation [12]

$$N(E_F) = \frac{3}{4\pi R^3 W} \quad (12)$$

and its values are of the order of $10^{20} \text{ eV}^{-1} \text{ cm}^{-3}$, as given in Table 2, which are reasonable for localized states [27,47].

The calculated values of W , N , R , r_p and $N(E_F)$ have been calculated using Eqs. (9),(10), (11) and (12) respectively and are listed in Table 2. These values are in the range as reported by many other researchers [11,12,20,21]. Perusal of the data presented in Table 2 shows that the activation energy (W) decreases with increase in conductivity, which is an expected result. The increase in conductivity and decrease in (W) with TMI content in the glass system may be attributed to decrease of the polaron hopping distance, R increases with increase in Fe_2O_3 content. A similar conclusion has been made by other researchers [48,49]. This may be due to the fact that in the present system the mole percentage of SiO_2 is constant and smaller Fe^{3+} ions replaces bigger Bi^{3+} ions.

3.2.1. Variable range hopping (VRH) model

N.F. Mott and E.A. Davis [41] has proposed a variable-range hopping (VRH) conduction, generally used to explain three dimensional (3-D) VRH in bulk disordered semiconductors, in low temperature range. However, Greaves [50] suggested the applicability of Mott's VRH in high temperature region with some modifications.

It is observed that plots of $\log \sigma_{dc}$ versus $T^{-1/4}$ (shown in Fig. 8) give better linear fit (with linearity ~ 0.9998) in comparison to the respective Arrhenius plots ($\log \sigma_{dc}$ versus $1000/T$), which shows linearity ~ 0.9988 .

The Mott's VRH model is suitable for explaining the dc conductivity data of the present oxides glass at high temperature. Based on Mott's VRH model [51] with modifications as suggested by Greaves [50]; the dc conductivity for 3-D case is given by

$$\sigma_{dc} = A e^{-\left[\frac{B}{T^4} \right]} \quad (13)$$

Where A and B are constants, given by relations

$$A = v_{ph} e^2 N(E_F) R^2 \quad (14)$$

$$B = B_o \left[\frac{\alpha^3}{kN(E_F)} \right]^{\frac{1}{4}} \quad (15)$$

Where α is the inverse localization length of s-like wave function has been estimated from the slope of $\log \sigma_{dc}$ vs $T^{-1/4}$ graph by taking $B_0 = 2.1$ in Eq. (15)[50]. The calculated values of α (i.e. from Eq.15) lies in the range 0.585 to 0.841 which are in very good agreement with those suggested by Murawski et al.[52] for oxide glasses. It is observed that the equality $\alpha - 1 < r_p < R$ is found to hold in the whole studied temperature range, so the polaron theory is applicable [52] to the present glass compositions.

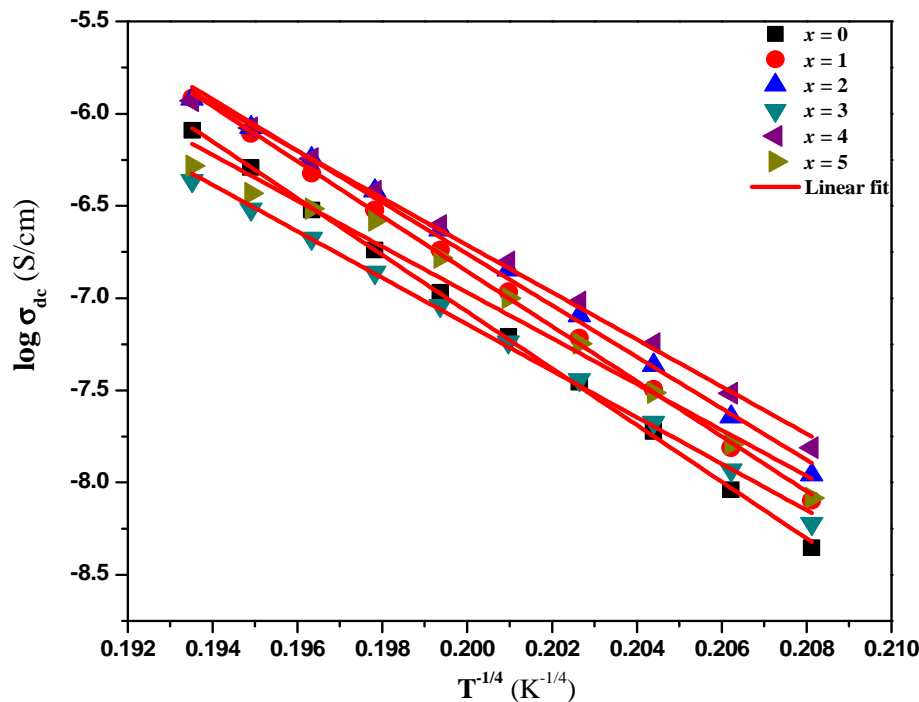


Fig.8. Plot of $\log \sigma_{dc}$ vs $T^{-1/4}$ for glass ceramics compositions $60\text{SiO}_2.(40-x)\text{Bi}_2\text{O}_3.x\text{Fe}_2\text{O}_3$. Where symbols represent experimental data and solid lines represents the linear fit.

CONCLUSION

The temperature dependence of ac and dc conductivity of studied glass ceramics compositions $60\text{SiO}_2.(40-x)\text{Bi}_2\text{O}_3.x\text{Fe}_2\text{O}_3$ with $x = 0, 1, 2, 3, 4$ and 5 were analyzed in the frame work of Jonscher's power law and variable range hopping model of Mott and Greave in the wide temperature range 533 K to 713 K and frequency range 10^{-1} Hz to 1MHz. It is observed that conductivity was found to increase with increase in Fe_2O_3 content. Various parameters like dc conductivity (σ_{dc}), cross-over frequency (ω_H) and frequency exponent (s) had been estimated from theoretical fitting of experimental data of ac conductivity with Jonscher's power law, which showed very good agreement for all the compositions. On addition of Fe_2O_3 in bismuth silicate glass ceramics system, the number of mobile charge carriers, at any instant was found less than the total number of charge carriers and the mobility of charge carriers was observed to increase with increase in Fe_2O_3 content. It was found that the correlated barrier hopping model was suitable to describe the conduction mechanism of present studied glass ceramic system, whereas, other models such quantum mechanical tunneling model and over lapping of large polarons model did not agree with the ac conductivity data and its frequency exponent of iron doped bismuth silicate glass ceramics. So, for the presently studied glass ceramics compositions Greaves VRH model was found to be in good agreement with the experimental data.

REFERENCES

- [1] J. Livage, J. P. Jollivet, E. Tronc, *J. Non-Cryst. Solids*, **1990**, 121, 35-39.
- [2] A. Ghosh, D. Chakravorty, *Appl. Phys. Lett.*, **1991**, 59, 855-856.
- [3] S. Mandal, A. Ghosh, *Phys. Rev. B*, **1994**, 49, 3131-3135.
- [4] A. Ghosh, D. Chakravorty, *Phys. Rev. B*, **1993**, 48, 5167-5171.
- [5] A. Ghosh, *Phys. Rev. B*, **1990**, 42, 5665-5676.
- [6] M. Sayer, A. Mansingh, *Phys. Rev. B*, **1972**, 6, 4629-4642.
- [7] A. Ghosh, *J. Appl. Phys.*, **1988**, 64, 2652-2655.
- [8] N.F. Mott, *J. Non-Cryst. Solids*, **1968**, 1, 1-17
- [9] A. Ghosh, S. Bhattacharya, A. Ghosh, *J. Phys. Condens. Matter.*, **2009**, 21, 145802.
- [10] A. Ghosh, S. Bhattacharya, D.P. Bhattacharya, A. Ghosh, *J. Phys. Condens. Matter.*, **2008**, 20, 035203.
- [11] R. Punia, R. S. Kundu, Meenakshi Dult, S. Murugavel and N. Kishore *J. Appl. Phys.*, **2012**, 112, 083701.
- [12] R. Punia, R. S. Kundu, S. Murugavel and N. Kishore *J. Appl. Phys.*, **2012**, 112, 113716.
- [13] N.F. Mott, *J. Non-Cryst. Solids*, **1968**, 1, 1-17.
- [14] I.G. Austin, N. F. Mott, *Adv. Phys.*, **1969**, 18, 41-102.
- [15] Y. Sakuri, J. Yamaki, *J. Electrochem. Soc.*, **1985**, 132, 512-513.
- [16] J. Lakshmana Rao, B. Sreedhar, M. Ramachandra Reddy, S.V.J. Lakshman, *J. Non-Cryst. Solids*, **1989**, 111, 228-237.
- [17] Sanjay, N Kishore and A. Agrawal, *Indian Journal Pure Appl. Phys.*, **2010**, 48, 205-211.
- [18] K. Trzebiatowski, J. Gackowska, W. Lizak, L. Muarwski, *Optica Applicata.*, **2005**, 35, 869-874.
- [19] S.K. Despande, V.K. Shrikhande, M.S. Jogad, P.S. Goyal, G.P. Kothiyal, *Bull. Mater. Sci.*, **2007**, 30, 497-502.
- [20] Meenakshi Dult, R.S. Kundu, S. Murugavel, R. Punia, N Kishore, *Physics B*, **2014**, 452, 102-107.
- [21] Meenakshi Dult, R.S. Kundu, J. Hooda, S. Murugavel, R. Punia, N Kishore, *J. Non-Cryst. Solids*, **2015**, 423-424, 1-8.
- [22] B.K. Chaudhuri, K. Chaudhuri and K.K. Som, *J. Phys. Chem. Solids*, **1989**, 50, 1137-1147.
- [23] B.K. Chaudhuri, K. Chaudhuri and K.K. Som, *J. Phys. Chem. Solids*, **1989**, 50, 1149-1155.
- [24] A. Ghosh *J. Appl. Phys.*, **1989**, 66, 2425-2429.
- [25] A. Ghosh *Phys. Rev. B*, **1990**, 42, 1388-1393.
- [26] Rajesh Parmar, R.S. Kundu, R. Punia, P. Aghamkar, N Kishore, *Physica B*, **2014**, 450, 39-44.
- [27] K.V. Ramesh, D.L. Sastry, *Phys. B*, **2007**, 387, 45-51.
- [28] M. Gabr, K.A. Ali, A.G. El-Din Mostafa, *Turk. J. Phys.*, **2007**, 31, 31-39,
- [29] K.H. Mahmoud, F.M. Abdel-Rahim, K. Atef, Y.B. Sadleek, *Curr. Appl. Phys.*, **2011**, 11, 55-60.
- [30] Sajjan Dahiya, Rajesh Punia, Anupinder Singh, Anup S. Maan and Sevi Murugavel, *J. Am. Ceram. Soc.* (**2015**), 49, 2776-2783.
- [31] A.K. Jonscher, *Dielectric Relaxation in Solids*, Chelsea Dielectrics, London, **1983**
- [32] A. Dutta, A. Ghosh, *Phys. Rev. B*, **2005**, 72, 224203.
- [33] J. C. Dyre and T. B. Schoder, *Rev. Mod. Phys.*, **2000**, 72, 873-892.
- [34] F.N. Abd El-Kader, A.M. Shehap, M.S. Abo Ellil, K.H. Mahmoud, *J. Polym. Mater.*, **2005**, 32, 349-356.
- [35] P.V. Rao, M.S. Reddy, V.R. Kumar, Y. Gandhi, N. Veeraiah, *Turk. J. Phys.*, **2008**, 32, 341-356.
- [36] H. Jain, J.N. Mundy, *J. Non-Cryst. Solids*, **1987**, 91, 315-323.
- [37] I.G. Austin and N. F. Mott, *Adv. Phys.*, **1969**, 18, 41-102.
- [38] S. R. Elliot, *Phil. Mag.*, **1977**, 36, 1291-1304.
- [39] S. R. Elliot, *Phil. Mag. B*, **1978**, 37, 553-560.
- [40] S. R. Elliot, *Adv. Phys.*, **1987**, 36, 135-217.
- [41] N. F. Mott and E. A. Davis, *Electronic Processes in Non-Crystalline Materials* (Oxford University Press, Oxford, 1979).
- [42] A. R. Long, *Adv. Phys.*, **1982**, 31, 553-637.
- [43] G.E. Pike, *Phys. Rev. B*, **1972**, 6, 1572-1579.
- [44] B.R. Springett, *J. Non-Cryst. Solids*, **1974**, 15, 179-190.
- [45] L.D. Raistrick, J.R. Macdonald, D.R. Franceschetti, J.R. Macdonald (Eds.), *Impedance Spectroscopy*, Wiley, New York, **1987**.
- [46] M. Cutroni, A. Mandanici, A. Piccolo, C. Fanggao, G.A. Saunders, P. Mustarelli, *Soild State Ionics*, **1996**, 90, 167-172.
- [47] P.N. Rao, D.K. Rao, N. Veeraiah, *Indian J. Engg. Mater. Sci.*, **2006**, 13, 69-74.
- [48] M. Pal, K. Hirota, Y. Tsujigami, H. Sakata, *J. Phys. D: Appl. Phys.*, **2001**, 34, 459-464.

- [49] H. Sakata, K. Segal, B.K. Chaudhari, *Phy. Rev. B*, **1999**, 60, 3230-3246.
[50] G.N Greaves, *J. Non-Cryst. Solids*, **1973**, 11, 427-446.
[51] A. Ghosh, *J. Chem. Phys.*, **1995**, 102, 1385.
[52] L. Murawski, C.H. Chung, J.D. Mackenzie, *J. Non-Cryst. Solids*, **1979**, 32, 91-104.